

Supporting information for article:

Twisting Induces Ferromagnetism in Homometallic Clusters

Ghenadie Novitchi,^{a*} Sergi Vela,^b Guillaume Pilet,^c Cyrille Train,^a Vincent Robert^{b*}

^a. *Laboratoire National des Champs Magnétiques Intenses, UPR CNRS 3228, Université Grenoble-Alpes, B.P. 166, 38042 Grenoble Cedex 9, France e-mail : ghenadie.novitchi@lncmi.cnrs.fr*

^b. *Institut de Chimie, UMR 7177 CNRS-Université de Strasbourg, 1 rue Blaise Pascal 67008 Strasbourg cedex, France, e-mail : vrobert@unistra.fr*

^c. *Laboratoire des Multimatériaux et Interfaces (UMR 5615), Université Claude Bernard Lyon 1, 69622 Villeurbanne Cedex, France*

Chemicals. All reagents were used as purchased from commercial suppliers. L-Proline and 4,4'-Diaminodiphenylmethane was from TCI EUROPE.

Physical Techniques. The FTIR spectra were obtained using the Nicolet Fourier Transform Infra-Red (FTIR) spectrophotometer iS 50 IR. The FTIR spectra were recorded in KBr pallets with 32 scans per spectrum at a resolution of 4 cm⁻¹. UV-vis absorption spectra were recorded on JASCO V770 spectrophotometer, while CD spectra on JASCO J1500 spectrometer. The spectra were measured at room temperature in a cuvette with 10 mm path length.

The ¹H, ¹³C NMR spectra were recorded on Bruker Avance II spectrometers at 300 (¹H) and 75.4 (¹³C) MHz, respectively. The ¹H and ¹³C chemical shifts were referred to the residual signals from the solvent as reference. Deuterated solvent DMSO-d₆ was from Sigma-Aldrich.

Variable-temperature (2.0-300 K) direct current (*dc*) and magnetic susceptibility and magnetization measurements were carried out on slightly crushed polycrystalline sample with a Quantum Design SQUID magnetometer. The *dc* susceptibility was measured using an applied field of 0.1 T. The magnetic susceptibility data were corrected for the diamagnetism of the constituent atoms and the sample holder contribution.^[1]

Synthesis

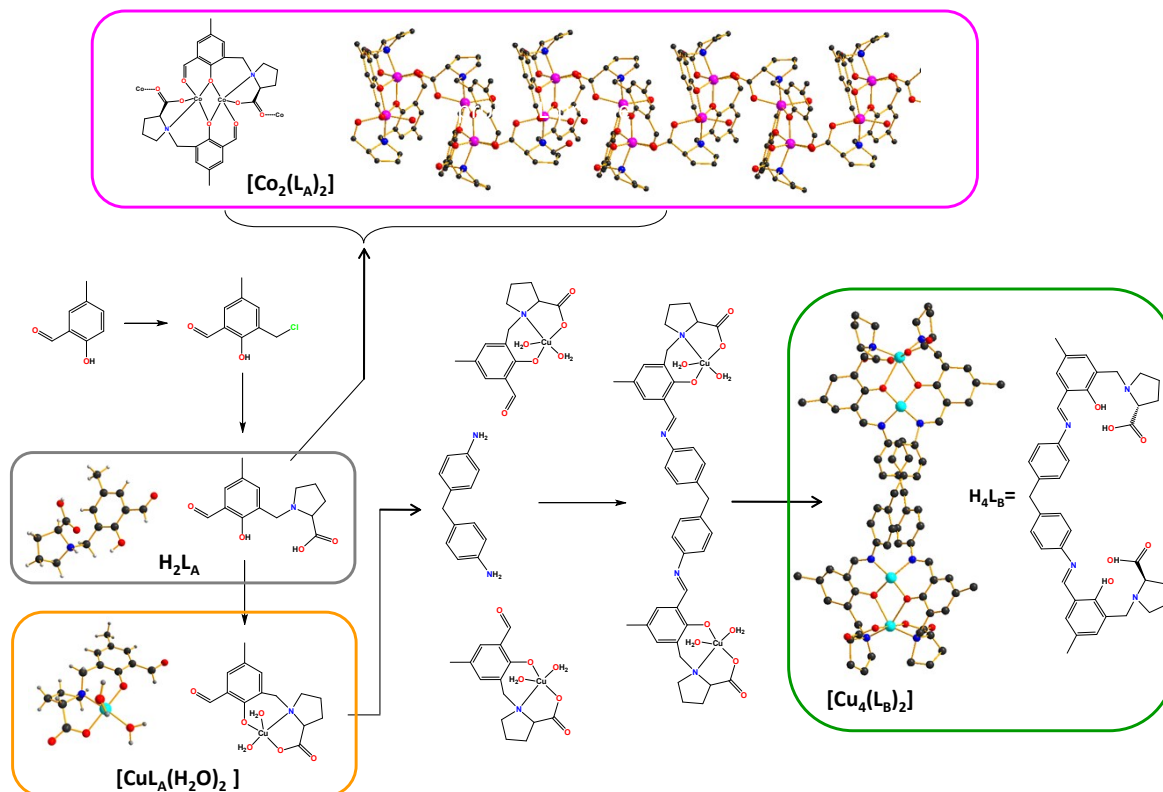


Figure S1. The scheme of synthesis of $\text{H}_2\text{L}_\text{A}$, $[\text{CuL}_\text{A}(\text{H}_2\text{O})_2]$, $[\text{Co}_2(\text{L}_\text{A})_2]$, and $[\text{Cu}_4(\text{L}_\text{B})_2]$ compounds.

General description: The 2-hydroxy-3-methyl-(*S*)-pyrrolidine-2-carboxylate-5-methylbenzaldehyde methyl ester was synthesized according to previously reported protocols.^[2] The hydrolysis reaction was performed in the base solution (10% NaOH) following by acidulation of solution (10% HCl) which lead to obtain the desired chiral ligand $\text{H}_2\text{L}_\text{A}$. Due to formations of zwitterions the acidulation procedure is difficult to manage because the acid base equilibrium generates different salts in solution. For X-ray analysis the crystal with composition $\text{H}_2\text{L}_\text{A} \cdot \{\text{H}_2\text{L}_\text{A} \cdot \text{HCl}\}$ have been eliminated at pH = 4. A non-acidulated form of $\text{H}_2\text{L}_\text{A}$ was obtained (in our case) at the pH~5 which are confirmed by NMR spectroscopy (see the integral ratio of large signal at 8.77 ppm assignment to the $\text{C}_{\text{Ph}}\text{-OH}$ and COOH protons Figure S2.). The obtained chiral ligand $\text{H}_2\text{L}_\text{A}$ easily interact with excess of freshly prepared $\text{Cu}_2(\text{OH})_2\text{CO}_3$ and CoCO_3 with elimination of CO_2 . Using the commercial carbonates make the reaction much longer and form sticky non crystalline products. The two different compounds have been obtained in the case of copper(II) and cobalt(II). The copper complex $[\text{CuL}_\text{A}(\text{H}_2\text{O})_2]$ has a mononuclear structure in which the coordination of ligand coordinate by deprotonated phenol group and deprotonated carboxylate group (Figure S7). The pentacoordinated environment of copper is completed by coordination of nitrogen of proline ring and two molecules of water. The aldehyde group is not involving in the coordination and used than in the condensation reaction with the 4,4'-diaminodiphenylmethane to form the tetranuclear cluster $[\text{Cu}_4(\text{L}_\text{B})_2]$. The L-proline fragment conserves its chiral configuration along all chemical transformation and consequently generates the

chiral helical shape of cluster $[\text{Cu}_4(\text{L}_\text{B})_2]$ (Figure S4, S7, S11). In contrast to copper at the similar condition the reaction of cobalt carbonate with $\text{H}_2\text{L}_\text{A}$ form the compound $[\text{Co}_2(\text{L}_\text{A})_2(\text{H}_2\text{O})] \cdot (\text{H}_2\text{O})$ in which the binuclear $\{\text{Co}_2\}$ units form the 1D coordination polymer (Figure S9) connected by carboxylate groups. The differences in the coordination function of deprotonated ligand $\text{H}_2\text{L}_\text{A}$ can be clearly see in the IR spectra (Figure S6). We didn't successes to interact the $[\text{Co}_2(\text{L}_\text{A})_2]$, with diaminodiphenylmethane, probably due to the insolubility of polymer chain and involving the aldehyde group in the coordination.

In order to obtained the $\text{H}_4\text{L}_\text{B}$ ligand we perform the condensation reaction between 4,4'-diaminodiphenylmethane and $\text{H}_2\text{L}_\text{A}$ in the ethanol (95%) in 1:2 molar ratio. As results we obtained the orange solids in which (according the ^1H NMR spectra) the aldehyde group is completely transformed into imine what supporting fact of formation of Schiff base. The infrared spectra of $\text{H}_4\text{L}_\text{B}$ have similar characteristic bands as in tetranuclear copper cluster $[\text{Cu}_4(\text{L}_\text{B})_2]$ (Figure S10). Unfortunately the ^1H NMR spectrum shows presence of additional signals probably impurity or molecules/ions from acid-base equilibrium. We actually working in order to perform the best conditions of this reaction and preceding of purification of $\text{H}_4\text{L}_\text{B}$.

2-hydroxy-3-methyl-(S)-pyrrolidine-2-carboxylate-5-methylbenzaldehyde ($\text{H}_2\text{L}_\text{A}$) The reaction of hydrolysis of ester have been done in 10% of NaOH and was precipitated by addition of 10% HCl (pH~5). The solution was completely evaporated and the crude product was recrystallized from $\text{CHCl}_3/\text{C}_2\text{H}_5\text{OH}$. The suitable for X-ray crystal have been growing from chloroform solution. ^1H NMR (300 MHz, CDCl_3) δ 9.93 (s, 1H), 8.75 (s, 2H), 7.54 (d, $J = 1.95\text{Hz}$, 1H), 7.42 (d, $J = 1.95\text{Hz}$, 1H), 4.28 (m, 2H), 3.86 (m, 1H), 3.53 (m, 1H), 2.93 (m, 1H), 2.45-1.97 (m, 5H), 1.97 (m, 2H). ^{13}C NMR (75 MHz, CDCl_3) δ 195.31, 156.90, 140.31, 134.32, 129.04, 119.65, 117.50, 57.07, 52.93, 50.11, 27.61, 21.71, 19.19, 17.37.

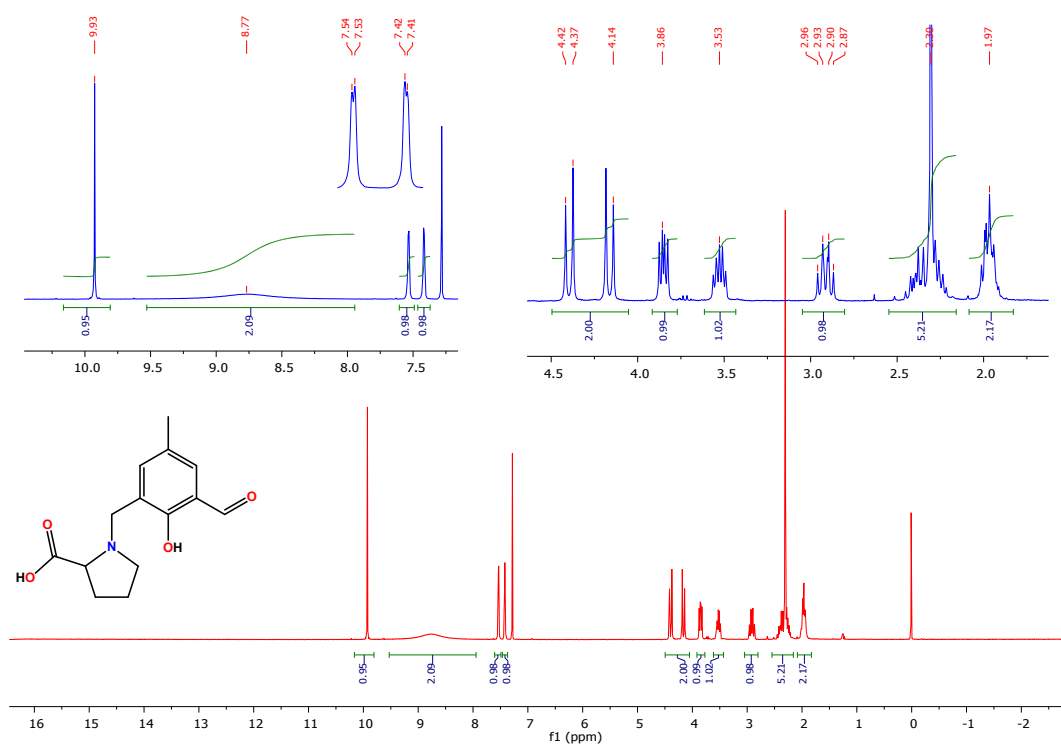


Figure S2. ^1H NMR spectra (300 MHz) of $\text{H}_2\text{L}_\text{A}$ in CDCl_3 at room temperature

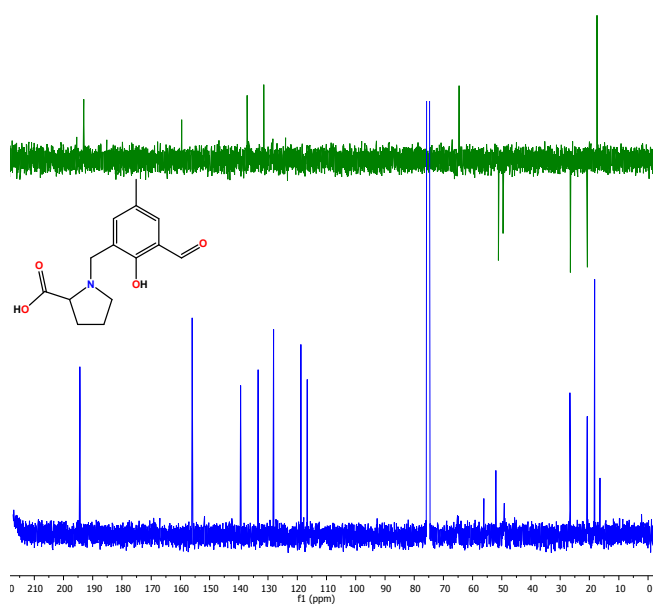


Figure S3. ^{13}C NMR spectra (75.4 MHz) of $\text{H}_2\text{L}_\text{A}$ in CDCl_3 at room temperature.

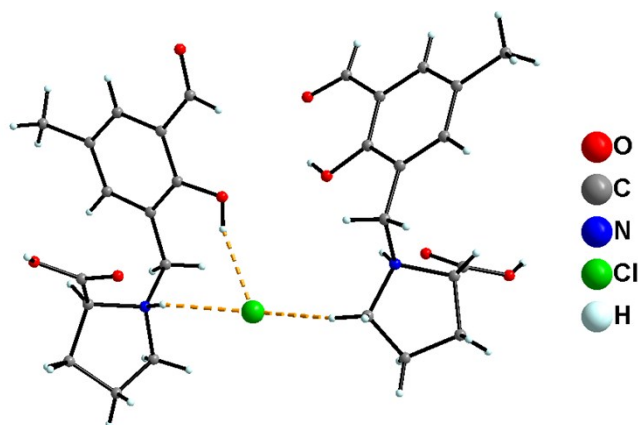


Figure S4 X-ray structure of $\text{H}_2\text{L}_\text{A}$

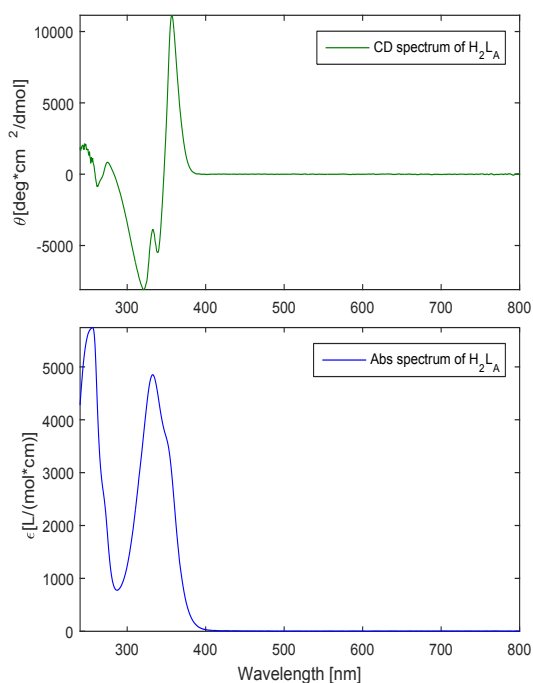


Figure S5. CD (top) and absorption (down) spectra of $\text{H}_2\text{L}_\text{A}$ in methanol solution.

[CuL_A(H₂O)₂] To a solution of 2-hydroxy-3-methyl-(*S*)-pyrrolidine-2-carboxylate-5-methylbenzaldehyde (0.63 g, 2 mmol) in Methanol (15 mL) under stirring an excess freshly prepared Cu₂(OH)₂CO₃ was added. The reaction mixture stirred was refluxed for 1 h. The obtained dark green solution was filtrated. Upon slow evaporation at the room temperature the crystals was formed during 2 days. The crystals was filtered off, washed with cold ether (5 mL) and dried in air. The suitable cristal for X-ray diffraction was fund from filtrated cristals. Yield: 0.25 g, 38.5%. Anal. Calcd for C₁₄H₁₉CuNO₆· (*M* 360.85 g mol⁻¹), %: C, 46.60; H, 5.31; N, 3.88. Found, %: C, 47.00; H, 5.25; N, 3.56.

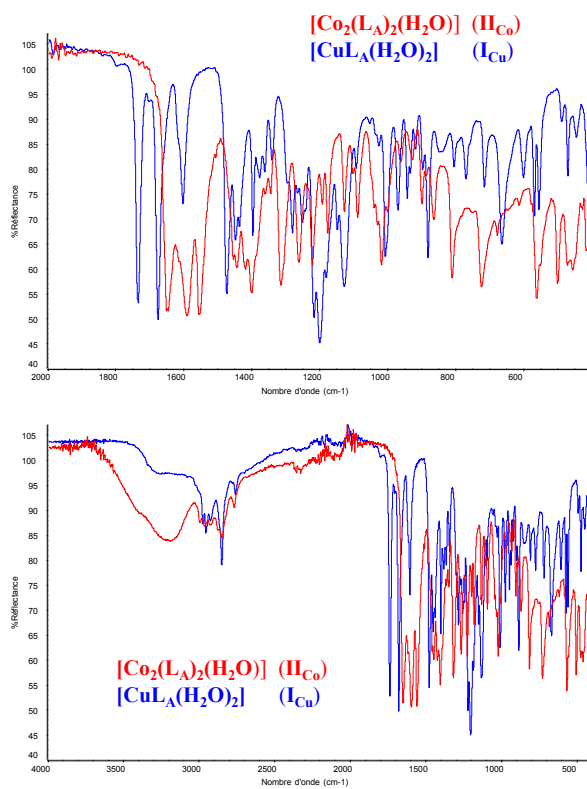


Figure S6 IR spectra for $[\text{CuL}_\text{A}(\text{H}_2\text{O})_2]$ and $[\text{Co}_2(\text{L}_\text{A})_2(\text{H}_2\text{O})]$

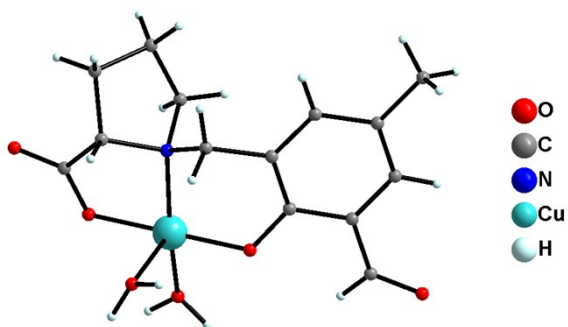


Figure S7 X-ray structure of $[\text{CuL}_\text{A}(\text{H}_2\text{O})_2]$

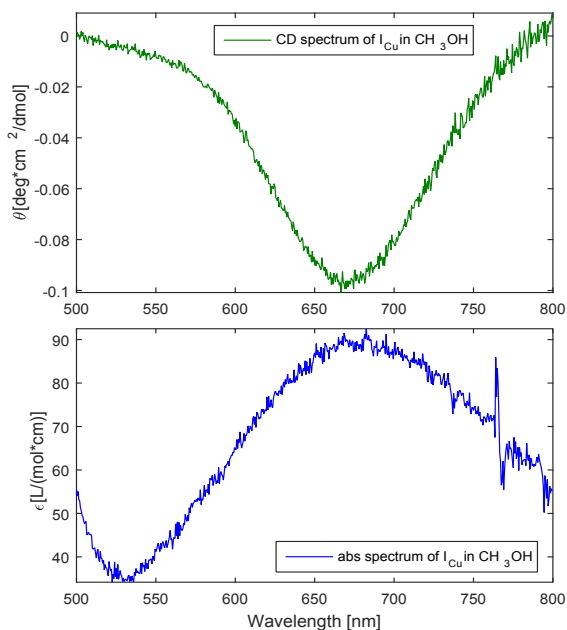


Figure S8 CD (top) and absorption (down) spectra of $[\text{CuL}_A(\text{H}_2\text{O})_2]$ in methanol solution.

$[\text{Co}_2(\text{L}_A)_2(\text{H}_2\text{O})] \cdot 2\text{CH}_3\text{OH}$ the similar procedure as I_{Cu} have been applied in order to obtain the cobalt compound. The excess of freshly prepared CoCO_3 was used. After partial evaporation of the solvent the pink red crystals have been formed. Yield: 0.4g, 54.05%. Anal. Calcd for $\text{C}_{28}\text{H}_{32}\text{Co}_2\text{N}_2\text{O}_9 \cdot 2\text{CH}_3\text{OH}$ (M 740.6 g mol^{-1}), %: C, 49.87; H, 5.58; N, 3.88. Found, %: C, 49.45; H, 5.63; N, 3.70.

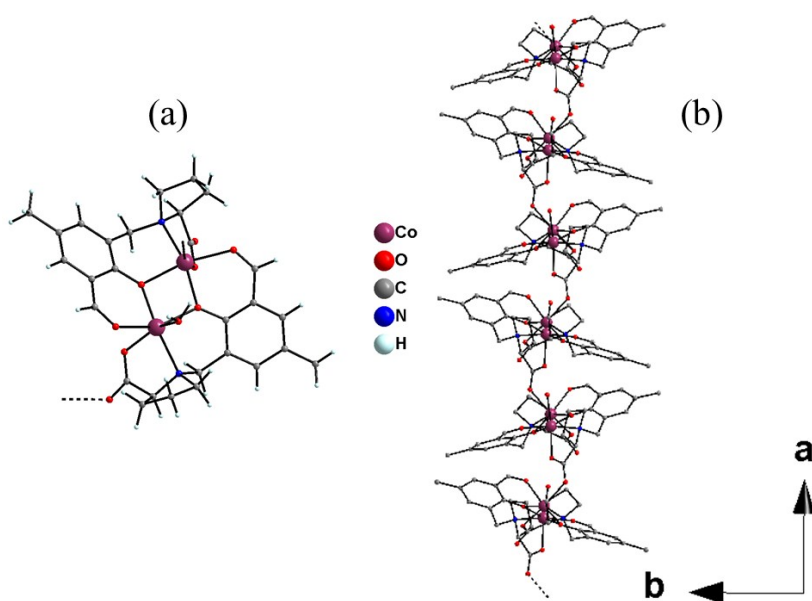


Figure S9 X-ray structure of $[\text{Co}_2(\text{L}_A)_2(\text{H}_2\text{O})] \cdot 2\text{CH}_3\text{OH}$

a) dinuclear core of $[\text{Co}_2(\text{L}_A)_2]$, b) chain of $[\text{Co}_2(\text{L}_A)_2]$, running along the a -axis of the unit-cell (for clarity non-coordinated solvent molecules and hydrogen atoms have been omitted).

$[\text{Cu}_4(\text{L}_B)_2] \cdot 6.5\text{CH}_3\text{OH} \cdot 6.5\text{H}_2\text{O}$ ($[\text{Cu}_4(\text{L}_B)_2]$) To the metanol solution (10 mL) of copper complexes $[\text{CuL}_A(\text{H}_2\text{O})_2]$ 0.185g (0.5 mmol) 0.05g (0.25mmol) of 4,4'-Diaminodiphenylmethane in 10 mL of CH_2Cl_2 was added. The obtained solution was stirred during 4h and then filtered from filter paper and left to crystallize by slow evaporation of solvent through the small hole in the cover. After a few days dark green crystals were formed which were separated and dried on filter paper. Yield: 0.4g, 54.05%. Anal. Calcd for $[\text{C}_{82}\text{H}_{80}\text{Cu}_4\text{N}_8\text{O}_{12}] \cdot 6.5\text{CH}_3\text{OH} \cdot 6.5\text{H}_2\text{O}$ (M 1949.11 g mol^{-1}), %: C, 54.53; H, 6.15; N, 5.75. Found, %: C, 58.03; H, 5.62; N, 6.29. (the misfitting of the elemental analysis is probably related to the solvent loss).

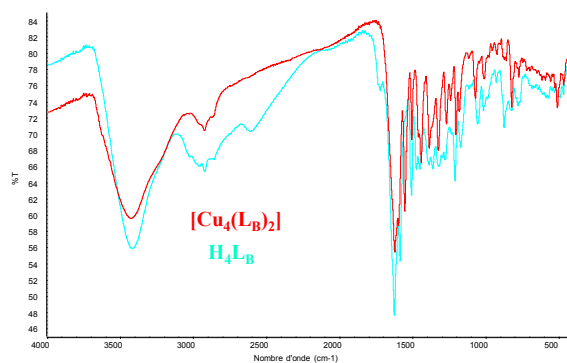


Figure S10 IR spectra for $[\text{Cu}_4(\text{L}_B)_2]$ and H_4L_B .

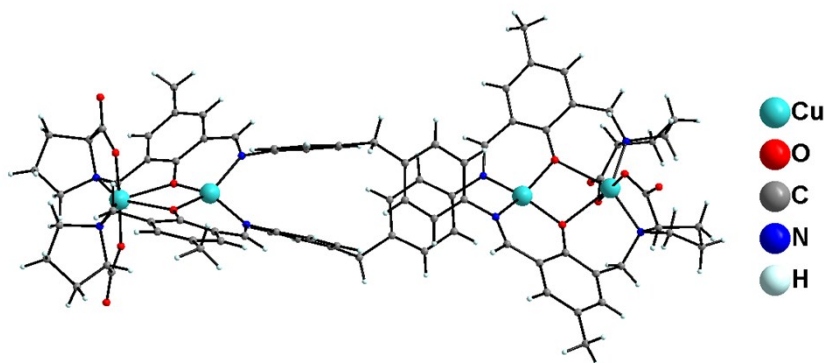


Figure S11. X-ray structure of $[\text{Cu}_4(\text{L}_B)_2] \cdot 6.5\text{CH}_3\text{OH} \cdot 6.5\text{H}_2\text{O}$

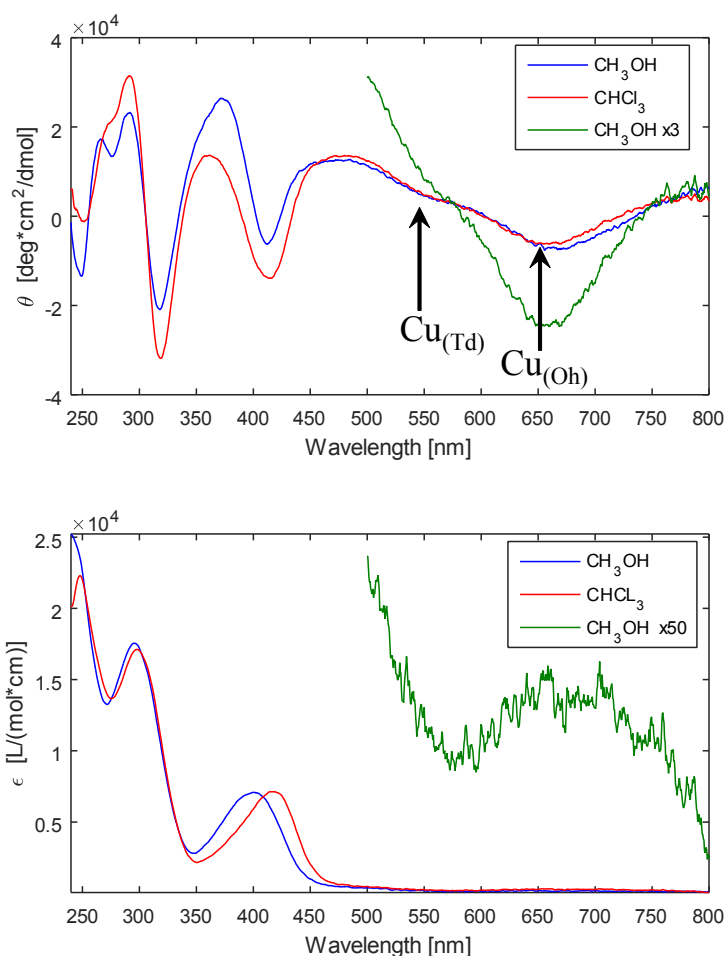


Figure S12. CD (top) and absorption (down) spectra of $[\text{Cu}_4(\text{L}_\text{B})_2]$ in methanol and chloroform solutions.

Experimental details of Crystallographic Structure Determination.

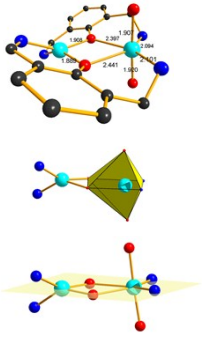
Single-crystal XRD studies of $[\text{CuL}_\text{A}(\text{H}_2\text{O})_2]$, $[\text{Co}_2(\text{L}_\text{A})_2]$ and $[\text{Cu}_4(\text{L}_\text{B})_2]$ were performed with a Gemini diffractometer and the related analysis software.^[3] Absorption corrections based on the crystal faces ^[4] (analytical, $[\text{Co}_2(\text{L}_\text{A})_2]$, and $[[\text{Cu}_4(\text{L}_\text{B})_2]$) and semi-empirical ^[5] (multi-scan, $\text{H}_2\text{L}_\text{A}$, $[\text{CuL}_\text{A}(\text{H}_2\text{O})_2]$) were applied to the data set. Structures were solved by direct methods with the SIR97 program ^[6] combined with Fourier difference syntheses and refined against F with the CRYSTALS program.^[7] All atomic displacement parameters for non-hydrogen atoms were refined with anisotropic terms. The hydrogen atoms were located theoretically on the basis of the conformation of the supporting atom and refined by using a riding model. All details are summarized in Table S1.

CCDC 1535638-1535641 contain the supplementary crystallographic data for structures $\text{H}_2\text{L}_\text{A}$, $[\text{CuL}_\text{A}(\text{H}_2\text{O})_2]$, $[\text{Co}_2(\text{L}_\text{A})_2]$ and $[\text{Cu}_4(\text{L}_\text{B})_2]$. These data can be obtained free of charge from the Cambridge Crystallographic Data Center (<http://ccdc.cam.ac.uk>).

Table S1. Single-crystal X-ray diffraction refinement details and results for $\text{H}_2\text{L}_\text{A}$ $[\text{CuL}_\text{A}(\text{H}_2\text{O})_2]$, $[\text{Co}_2(\text{L}_\text{A})_2]$ and $[\text{Cu}_4(\text{L}_\text{B})_2]$.

	$\text{H}_2\text{L}_\text{A}$	$[\text{CuL}_\text{A}(\text{H}_2\text{O})_2]$	$[\text{Co}_2(\text{L}_\text{A})_2]$	$[\text{Cu}_4(\text{L}_\text{B})_2]$
Formula	$\text{C}_{28}\text{H}_{35}\text{Cl}_1\text{N}_2\text{O}_8$	$\text{C}_{14}\text{H}_{19}\text{Cu}_1\text{N}_1\text{O}_6$	$\text{C}_{29.50}\text{H}_{40}\text{Co}_2\text{N}_2\text{O}_{11.50}$	$\text{C}_{88.50}\text{H}_{118.50}\text{Cu}_4\text{N}_8\text{O}_{25}$
Formula weigh (g.mol ⁻¹)	563.1	360.9	724.5	1948.6
Crystal system	Triclinic	Orthorhombic	Orthorhombic	Monoclinic
Space group	P1	$\text{P}2_12_12_1$	$\text{P}2_12_12_1$	$\text{P}2_1$
a (Å)	5.6286(6)	7.1420(9)	11.580(2)	13.9452(6)
b (Å)	10.261(2)	10.897(2)	12.053(2)	15.3362(5)
c (Å)	12.817(2)	18.928(3)	22.060(5)	21.8663(8)
α (deg.)	73.67(1)	90	90	90
β (deg.)	87.75(1)	90	90	89.343(3)
γ (deg.)	88.35(1)	90	90	90
V (Å ³)	709.7(2)	1473.1(3)	3079.0(8)	4676.1(2)
Z	1	4	4	2
Density	1.317	1.631	1.563	1.384
μ (mm ⁻¹)	0.186	1.515	1.143	0.974
Crystal size (mm ³)	0.10×0.13×0.14	0.09×0.10×0.11	0.03×0.11×0.17	0.10×0.27×0.45
Crystal shape	Block	Block	Needle	Plate
Crystal color	Colorless	Blue	Orange	Dark green
T (K)	293	293	110	110
No. ind. refl. [R_{int}]	3303 [0.034]	2098 [0.054]	7185 [0.124]	23180 [0.049]
$I/\sigma(I)$	3	3	2	23180
No. refl. used	2981	2001	3314	19548
No. ref. parameters	353	200	416	1163
R / R_w	0.0474 / 0.0512	0.0379 / 0.0396	0.0680 / 0.0758	0.0471 / 0.054
S	1.07	1.11	1.11	1.03
$\Delta\rho_{\text{max}} / \Delta\rho_{\text{min}}$ (e ⁻ .Å ⁻³)	+0.22 / -0.22	+0.59 / -0.66	+0.72 / -1.03	+1.12 / -1.00
Flack parameter	-0.1(1)	0.05(2)	-0.02(4)	0.045(7)
Absorption correction	Multi-scan	Multi-scan	Analytical	Analytical

Table S2. Important bond lengths and angles within the complex architecture.

	Dimer A	Dimer B
	$\text{Cu}_{\text{Td}}\text{-O}_{\text{Ph}}\text{-Cu}_{\text{Oh}} = 104.2^\circ$	$\text{Cu}_{\text{Td}}\text{-O}_{\text{Ph}}\text{-Cu}_{\text{Oh}} = 104.34^\circ$
	$\text{Cu}_{\text{Td}}\text{-O}_{\text{Ph}}\text{-Cu}_{\text{Oh}} = 103.15^\circ$	$\text{Cu}_{\text{Td}}\text{-O}_{\text{Ph}}\text{-Cu}_{\text{Oh}} = 103.88^\circ$
	$\text{Cu}_{\text{Td}}\text{-O} = 1.889 \text{ \AA}$	$\text{Cu}_{\text{Td}}\text{-O} = 1.896 \text{ \AA}$
	$\text{Cu}_{\text{Td}}\text{-O} = 1.908 \text{ \AA}$	$\text{Cu}_{\text{Td}}\text{-O} = 1.921 \text{ \AA}$
	$\text{Cu}_{\text{Td}}\text{-N} = 1.962 \text{ \AA}$	$\text{Cu}_{\text{Td}}\text{-N} = 1.985 \text{ \AA}$
	$\text{Cu}_{\text{Td}}\text{-N} = 1.950 \text{ \AA}$	$\text{Cu}_{\text{Td}}\text{-N} = 1.947 \text{ \AA}$
	$\text{Cu}_{\text{Oh}}\text{-O} = 1.920 \text{ \AA}$	$\text{Cu}_{\text{Oh}}\text{-O} = 1.931 \text{ \AA}$
	$\text{Cu}_{\text{Oh}}\text{-O} = 1.907 \text{ \AA}$	$\text{Cu}_{\text{Oh}}\text{-O} = 1.917 \text{ \AA}$
	$\text{Cu}_{\text{Oh}}\text{-N} = 2.094 \text{ \AA}$	$\text{Cu}_{\text{Oh}}\text{-N} = 2.072 \text{ \AA}$
	$\text{Cu}_{\text{Oh}}\text{-N} = 2.101 \text{ \AA}$	$\text{Cu}_{\text{Oh}}\text{-N} = 2.101 \text{ \AA}$
	$\text{Cu}_{\text{Oh}}\text{-O} = 2.397 \text{ \AA}$	$\text{Cu}_{\text{Oh}}\text{-O} = 2.385 \text{ \AA}$
	$\text{Cu}_{\text{Oh}}\text{-O} = 2.441 \text{ \AA}$	$\text{Cu}_{\text{Oh}}\text{-O} = 2.419 \text{ \AA}$

Theoretical Details

In the light of the crystal structure, one can anticipate that magnetic interaction in $[\text{Cu}_4(\text{L}_\text{B})_2]$ is originate from two independent Cu_2 subunits referred to as **A** and **B** in the following. To support such statement, density functional theory (DFT) inspections were carried out on the whole structure to justify the absence of coupling between the Cu_2 units. Each Cu^{2+} ion being a $s = 1/2$ spin center, a $|M_\text{S}(\mathbf{A}) = 1 ; M_\text{S}(\mathbf{B}) = 1\rangle$ solution was first converged (energy E_Q). Despite the unrestricted character of the calculation, this solution is very similar to the $S=2$ pure quintet spin state, as reflected by the absence of spin contamination ($\hat{S}^2 = 6.00$). Then, by flipping the spins orientations on one Cu_2 unit (say **B** unit), the energy E_BS of the broken-symmetry solution $|M_\text{S}(\mathbf{A}) = 1 ; M_\text{S}(\mathbf{B}) = -1\rangle$ was calculated. The quasi-degeneracy of these two solutions, $\Delta E = |E_\text{BS} - E_\text{Q}| = 0.18 \text{ cm}^{-1}$, supports their independence from a magnetic point of view, and validates the intuitive picture of two non-interacting Cu_2 pairs. Within the material, the shortest $\text{Cu}\cdots\text{Cu}$ distance between two neighbouring tetranuclear complexes is 7.6 \AA . Therefore one can as well anticipate a negligible exchange coupling constant between tetranuclear units. All DFT calculations were carried out at the UB3LYP/6-31G(d) level as implemented in Gaussian 09.^[8] From this preliminary inspection, the Cu_4 compound was split into two Cu_2 moieties (see Figure S13). The carbon atoms environments were saturated with hydrogen atoms using standard C-H bond distances.

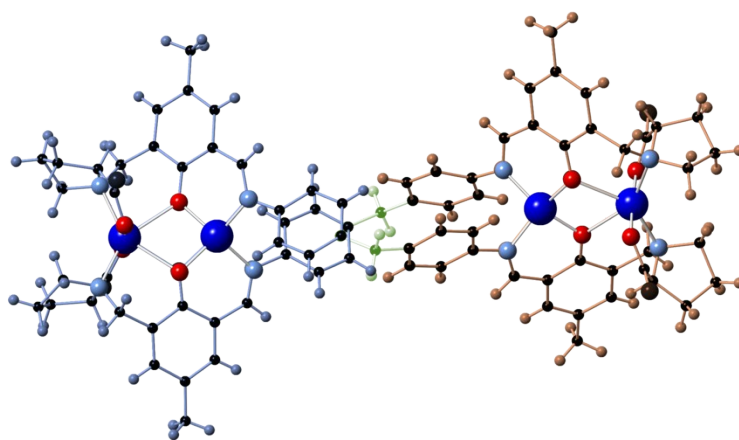


Figure S13. $[\text{Cu}_4(\text{L}_\text{B})_2]$ splitted into **A** (left, blue) and **B** (right, orange) architectures. The central methylene groups (green) were transformed into hydrogen atoms.

Based on these structures, wavefunction theory-based calculations were performed to examine the nature and amplitude of the magnetic interactions within both Cu_2 subunits. In the presence of two unpaired electrons in a Cu_2 unit, low-lying singlet (total spin $S=0$) and triplet ($S=1$) states are expected to compete. The energy difference defines the so-called exchange coupling constant $2J = E(S=0) - E(S=1)$ ruling the Heisenberg spin-Hamiltonian $\hat{H} = -2J\hat{S}_1\hat{S}_2$, \hat{S}_1 and \hat{S}_2 being the spin operators

defined on each Cu^{2+} ion. A natural strategy is to perform complete active space self-consistent field (CASSCF) calculations including two electrons in two molecular orbitals (MOs), namely CAS[2,2]SCF. As expected, the magnetic orbitals are the singly occupied MOs (SOMOs) of a d^9 ions in O_h and T_d environments, respectively (see Figure S15). All our calculations were performed within the MolCAS 8.0 package.^[9] The copper ions were described with a ANO-RCC type contraction (21s15p10d6f4g2h)/[4s3p2d1f]. Their nearest-neighbor nitrogen and oxygen atoms were described with DZP basis sets of ANO-RCC type ((14s9p4d3f2)/[3s2p1d]). To reduce the computational cost, carbon and hydrogen atoms were depicted with DZ ((14s9p4d3f2g)/[2s2p]) and minimal basis sets ((8s)/[1s]), respectively.

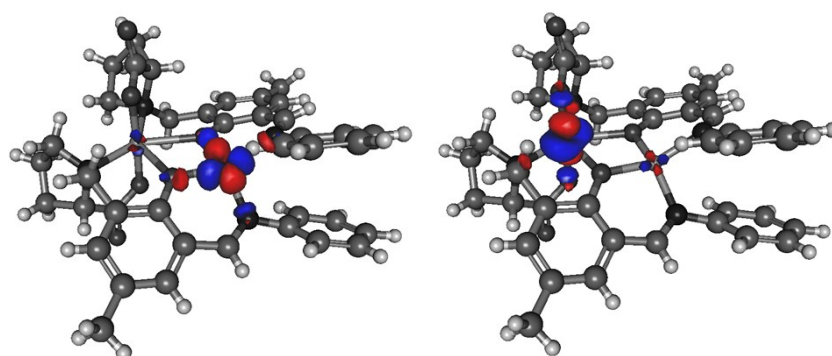


Figure S14. Active MOs extracted from a CAS[2,2]SCF calculation for the triplet state on fragment **A**. The active MOs on fragment **B** are very similar.

However, exchange interactions cannot be accurately evaluated ignoring the dynamical correlation contribution, and call for expansion that goes beyond a bare-valence picture. As a matter of fact, spectroscopic accuracy calls for larger configurations interactions expansions. Thus, for all inspected geometries, such effects were included using the DDCI (Difference Dedicated Configuration Interaction) method as implemented in the CASDI code.^[10] The methodology was reported in the literature and relies on a single set of MOs to describe the different spin states.^[11] Let us briefly recall that the classes of determinants are labeled following the number of excitations (holes, h, and/or particles, p) generated on top of the reference CAS wavefunction. First, we checked that the chosen set of MOs has a small impact on the calculated energy difference (less than 1 cm^{-1}). Thus, the successive levels (so-called CAS+S, and DDCI-3) were applied using the MOs of the triplet CAS[2,2]SCF solution (the DDCI-3 value is changed by less than 1.5 cm^{-1} when the CAS[2,2]SCF singlet MOs are used). The CAS+S level generates all single excitations and affords for a more realistic evaluation of the charge transfers between the Cu^{2+} ions and the inclusion of the spin polarization contributions. The former are negligible as soon as the singlet wavefunction is dominated by the neutral forms (*i.e.*, one electron in each active MOs). In contrast, the sign of the latter cannot be predicted *a priori* and

originates versatile magnetic behaviours. Let us mention that the DDCI-3 level calls for an expansion of the wavefunction over *ca.* 150 millions Slater determinants. Thus, we used the latest version of the CASDI code which takes advantage of the Cholesky decomposition.^[10]

- [1] a) O. Kahn, *Molecular Magnetism*, VCH Publishers, Inc., New York, Weinheim, Cambridge, **1993**, p;
b) P. Pascal, *Annales De Chimie Et De Physique* **1910**, *19*, 5-70.
- [2] a) M. N. M. Milunovic, E. A. Enyedy, N. V. Nagy, T. Kiss, R. Trondl, M. A. Jakupec, B. K. Keppler, R. Krachler, G. Novitchi and V. B. Arion, *Inorganic Chemistry* **2012**, *51*, 9309-9321; b) A. Dobrova, S. Platzer, F. Bacher, M. N. M. Milunovic, A. Dobrov, G. Spengler, E. A. Enyedy, G. Novitchi and V. B. Arion, *Dalton Transactions* **2016**, *45*, 13427-13439.
- [3] *CrysAlisPro*, v. 1.171.33.46 (rel. 27-08-2009 *CrysAlis171.NET*), Oxford Diffraction Ltd., **2009**, p.
- [4] J. Demeulenaer and H. Tompa, *Acta Crystallographica* **1965**, *19*, 1014-+.
- [5] R. H. Blessing, *Acta Crystallographica Section A* **1995**, *51*, 33-38.
- [6] A. Altomare, M. C. Burla, M. Camalli, G. L. Casciarano, C. Giacovazzo, A. Guagliardi, A. G. G. Moliterni, G. Polidori and R. Spagna, *Journal of Applied Crystallography* **1999**, *32*, 115-119.
- [7] D. J. Watkin, Prout, C. K., Carruthers, J. R., Betteridge, P. W. in *CRISTAL Issue 11, Vol. CRISTAL Issue 11*, Chemical Crystallography Laboratory, Oxford, UK, **1999**.
- [8] M. Frisch, G. Trucks, H. Schlegel, G. Scuseria, M. Robb, J. Cheeseman, G. Scalmani, V. Barone, B. Mennucci and G. Petersson in *Gaussian 09, revision D. 01, Vol. Gaussian, Inc., Wallingford CT*, **2009**.
- [9] B. O. Roos, R. Lindh, P. A. Malmqvist, V. Veryazov and P. O. Widmark, *Journal of Physical Chemistry A* **2005**, *109*, 6575-6579.
- [10] N. Ben Amor and D. Maynau, *Chemical Physics Letters* **1998**, *286*, 211-220.
- [11] J. P. Malrieu, R. Caballol, C. J. Calzado, C. de Graaf and N. Guihery, *Chemical Reviews* **2014**, *114*, 429-492.